Supporting Information

Conrady *et al.* 10.1073/pnas.0807717105

SI Text

Analytical Ultracentrifugation (AUC). All AUC experiments were performed at 20°C in a Beckman XL-I analytical ultracentrifuge using absorbance optics. Sedimentation velocity was performed at 47,000 rpm and the data were analyzed with Sedfit using a continuous c(s) distribution model (1). Sedimentation coefficients were also determined using the program Svedberg (2) and were converted to standard conditions ($s^0_{20,w}$) by extrapolation to infinite dilution and correction for solution conditions as described (3). Sedimentation equilibrium data were collected for Brpt1.5 (loading concentrations of 5–15 μM) at speeds of 20,000, 24,000, 35,000, and 47,000 rpm, and for Brpt1.5 (2–5 μM) at 15,000, 18,000, 20,000, 26,000, and 37,000 rpm. Monomer characterization and divalent cation screening were performed in 20 mM Tris pH 7.4, 150 mM NaCl (TBS), with 10 mM of the relevant chloride salt for the divalent cation screen. For $ZnCl_2$ titration experiments, samples were dialyzed into TBS with 0, 0.1, 0.3, 1, 2, 5, 8, or 10 mM Zn^{2+}. pH experiments were performed in 20 mM Tris, 20 mM MES, 50 mM NaCl with 10 mM $ZnCl_2$ adjusted to the appropriate pH. Dimer $s^0_{20,w}$ characterization was performed in 20 mM Tris pH 7.4, 50 mM NaCl, 10 mM Zn^{2+}. The equilibrium data were truncated in WinReedit and fitted globally with WinNonlin (www.rasmb.bbri.org/). The weight-averaged reduced buoyant molecular weight, σ_w, was determined followed by analysis of the monomer–dimer equilibrium. Calculation of the experimental molecular weights from σ, determination of the monomer–dimer equilibrium constants, and conversion of equilibrium constants into molar units were carried out as described (3, 4).

Data Analysis. The net number of protons or Zn^{2+} ions taken up or released upon dimerization was determined by analysis of the relevant linked equilibria. Briefly, when an equilibrium event, such as dimerization, is dependent on a solute molecule Y, one can plot the logarithm of the association constant for dimerization as a function of log[Y] to determine $\frac{(\delta \log K)}{(\delta \log[Y])} = \Delta Y$, where ΔY is the net number of Y molecules bound or released upon dimerization (5). The slope of the log K vs. log[Zn] plot was determined by linear regression to yield the net number of Zn^{2+} ions bound in the dimer interface. Likewise, the slope of the log K vs. log[H^+] plot was determined to give the net number of protons taken up or released upon association.

Sedimentation equilibrium-derived relative molecular weight data were fit in Scientist (Micromath Scientific Software) to a modified Hill equation of the form:

$$y = M_0 + \frac{(M_{max} - M_0)K^{n_H}x^{n_H}}{1 + K^{n_H}x^{n_H}},$$

where y is the relative molecular weight, x is the concentration of Zn^{2+}, M_o and M_{max} correspond to the relative molecular weights of monomer and dimer, respectively, K is the apparent association constant (i.e., $EC_{50}{}^{-1}$), and n_H is the Hill coefficient. The concentration of Zn^{2+} that yields 50% dimer (EC_{50}) was determined by taking the reciprocal of K. This equation was further modified to fit the pH variation data as follows:

$$y = M_0 + \frac{(M_0 - M_{max})(10^{pK_a - pH})^{n_H}}{1 + (10^{pK_a - pH})^{n_H}}.$$

In this case, the apparent pK_a is the pH at which 50% dimerization occurs, and the $(M_o - M_{max})$ term is inverted because the data show a dimer-to-monomer transition upon increase in proton concentration.

1. Schuck P (2000) Size-distribution analysis of macromolecules by sedimentation velocity ultracentrifugation and lamm equation modeling. *Biophys J* 78:1606–1619.
2. Philo JS (1997) An improved function for fitting sedimentation velocity data for low-molecular-weight solutes. *Biophys J* 72:435–444.
3. Herr AB, White CL, Milburn C, Wu C, Bjorkman PJ (2003) Bivalent binding of IgA1 to FcαRI suggests a mechanism for cytokine activation of IgA phagocytosis. *J Mol Biol* 327:645–657.
4. Herr AB, Ornitz DM, Sasisekharan R, Venkataraman G, Waksman G (1997) Heparin-induced self-association of fibroblast growth factor-2. Evidence for two oligomerization processes. *J Biol Chem* 272:16382–16389.
5. Wyman J, Gill SJ (1990) *Binding and Linkage: Functional Chemistry of Biological Macromolecules* (University Science Books, Mill Valley, CA).
6. Diaz C, Lopez F, Henriquez P, Rodriguez E, Serra-MaJem L (2001) Serum manganese concentrations in a representative sample of the Canarian population. *Biol Trace Elem Res* 80:43–51.
7. Ueno K, Imamura T, Cheng KL (1992) *Handbook of Organic Analytical Reagents* (CRC Press, Boca Raton, FL).

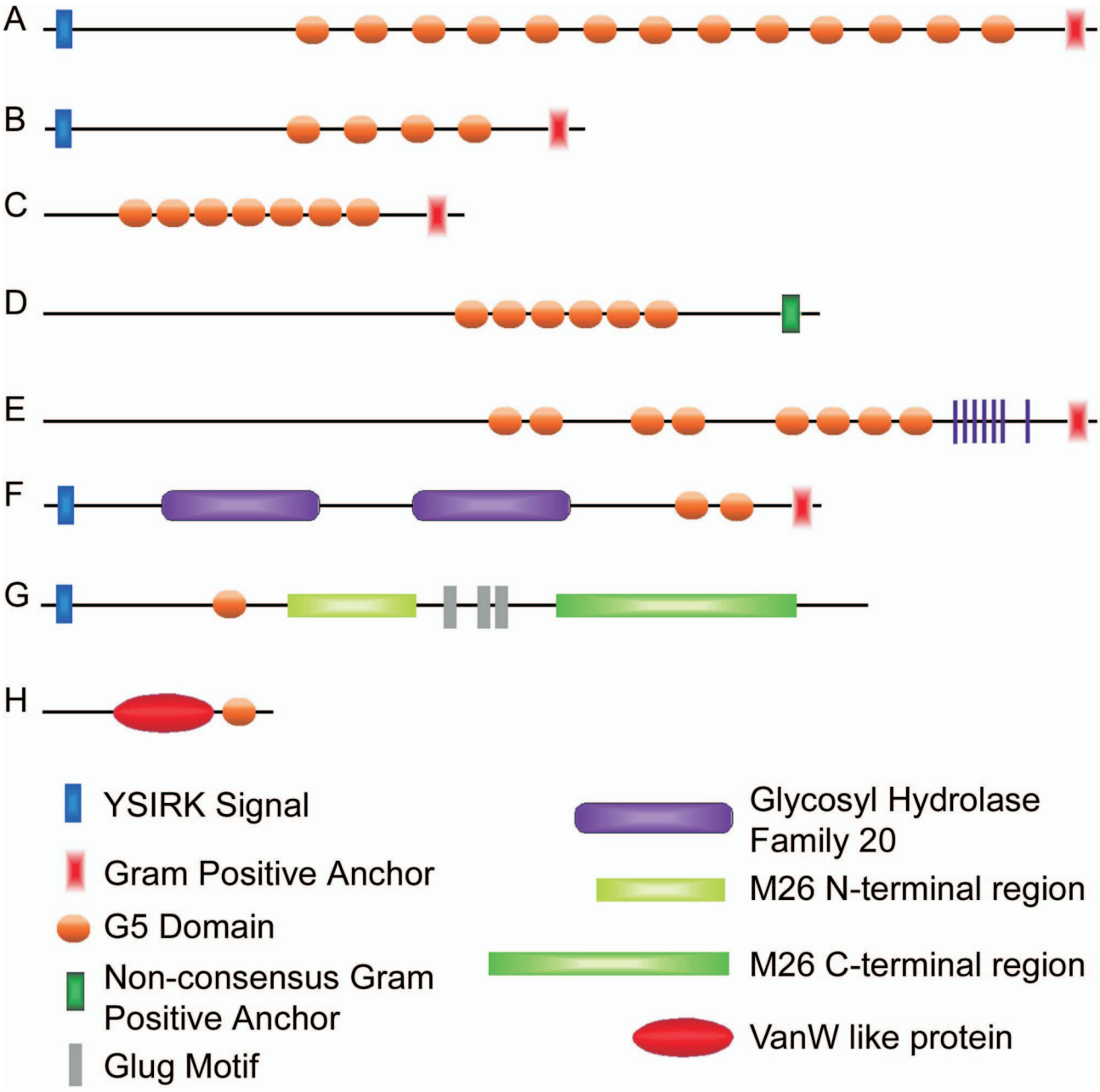

Fig. S1. Schematic of representative proteins containing multiple G5 domains identified by Pfam and Blast searches. (*A*) Aap from *S. epidermidis* strain RP62A. Similar architecture is observed in *S. aureus* proteins SasG and Pls, with the reported number of G5 repeats across Staphylococcal species varying from 4 to 17. (*B*) ''Surface protein from gram-positive cocci'' from *Streptococcus suis* 89/1591. (*C*) ''LPXTG cell wall surface protein'' from *Streptococcus gordonii* str. challis substr. ch1. (*D*) ''Putative cell surface protein precursor'' from *Corynebacterium urealyticum*. (*E*) ''Conserved hypothetical protein'' from *Fingoldia magna*. (*F*) β-N-acetylhexosaminidase from *Streptococcus pneumoniae*. Similar domain architecture is reported in various *S. pneumoniae* strains. (*G*) IgA1 protease from *S. pneumoniae*. Similar domain architecture is reported in predicted zinc metalloproteases from *S. pneumoniae*, *S. gordonii*, and *S. suis*, with up to four repeats of the G5 domain before the N-terminal peptidase domain. (*H*) VanW vancomycin resistance protein from *Thermosinus carboxydivorans*. Similar proteins are found in *Clostridium botulinum* and *C. difficile*, *Desulfotomaculum reducens*, *Caldicellulosiruptor saccharoluticus*, *Pelotomaculum thermopropionicum*, *Eubacterium ventriosum*, *Alkaliphilus* sp., *Thermonanaerobacter* sp., *Desulfitobacterium hafniense*, *Moorella thermoacetica*, *Carboxydothermus hydreogenoformans*, and *Symbiobacterium thermophilum*.

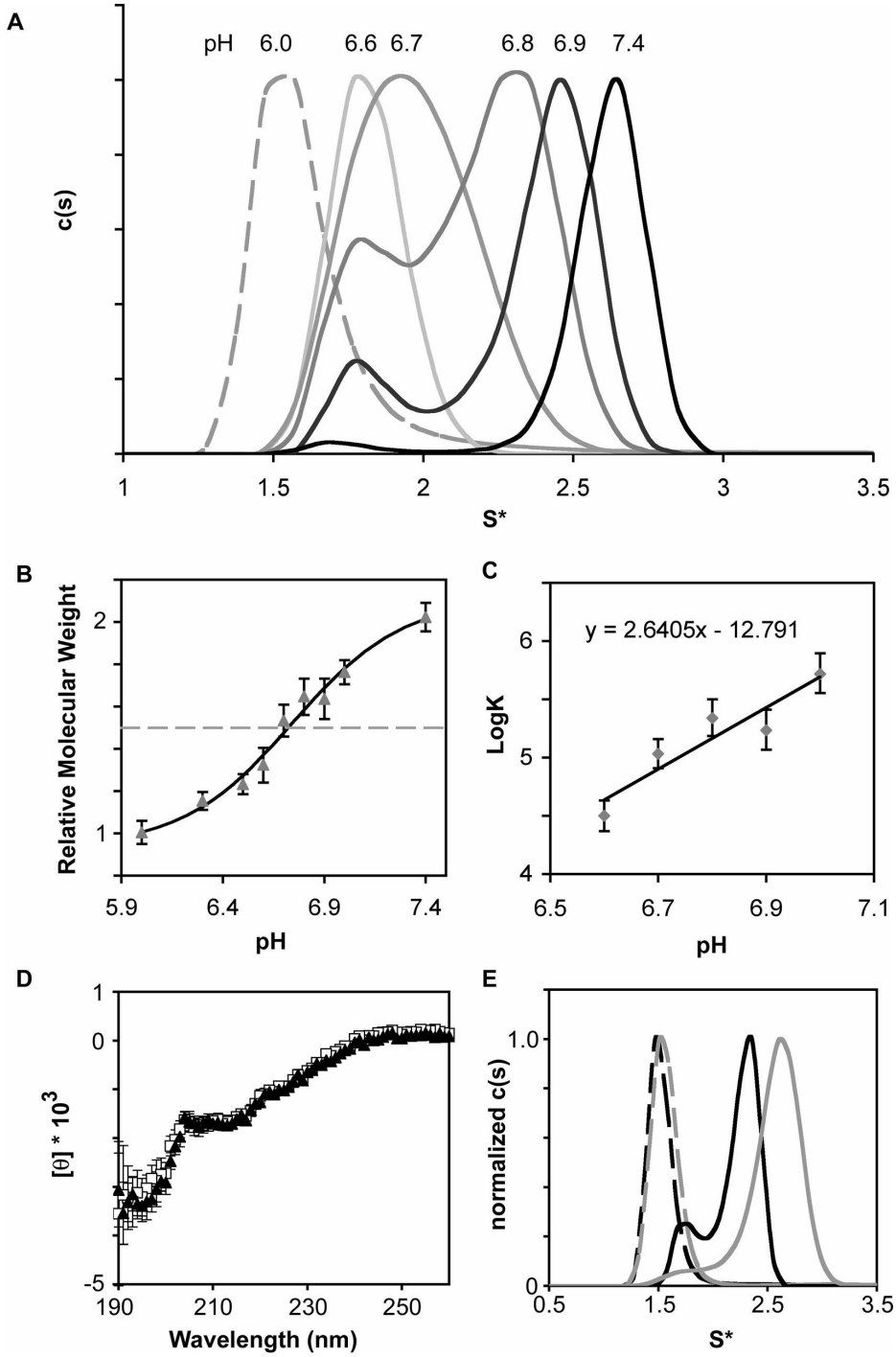

Fig. S2. pH dependence of Zn^{2+}-mediated G5 dimerization. (*A*) Sedimentation velocity analysis of the Zn^{2+}-dependent dimerization of Brpt1.5 as a function of pH in 20 mM Tris, 20 mM MES, 50 mM NaCl, and 10 mM $ZnCl_2$. Brpt1.5 shifts from dimer at pH 7.4 to monomer at pH 6.0. (*B*) Sedimentation equilibrium confirms that Brpt1.5 transitions from dimer to monomer as the pH is lowered from 7.4 to 6.0. The apparent pK_a of this transition is 6.7, which may indicate involvement of histidine residues in Zn^{2+}-dependent dimerization. (*C*) Linked equilibrium analysis of the pH dependence of Brpt1.5 dimerization at 10 mM $ZnCl_2$. The slope of the log *K* vs. log[H^+] plot, determined by linear regression, reveals that Brpt1.5 dimerization is linked to the release of ≈2 or 3 protons. (*D*) Far-UV CD spectrum of the H75A/H85A Brpt1.5 mutant in the presence (squares) and absence (triangles) of 10 mM $ZnCl_2$. (*E*) Sedimentation velocity analysis of wild-type Brpt1.5 (gray) compared to histidine-null mutant H75A/H85A (black). Dashed lines show data collected in the absence of Zn^{2+}, and solid lines show data collected at 10 mM $ZnCl_2$. Partial loss of dimerization is observed in the H75A/H85A mutant, suggesting that one or both histidines and other residues are involved in Zn^{2+} coordination.

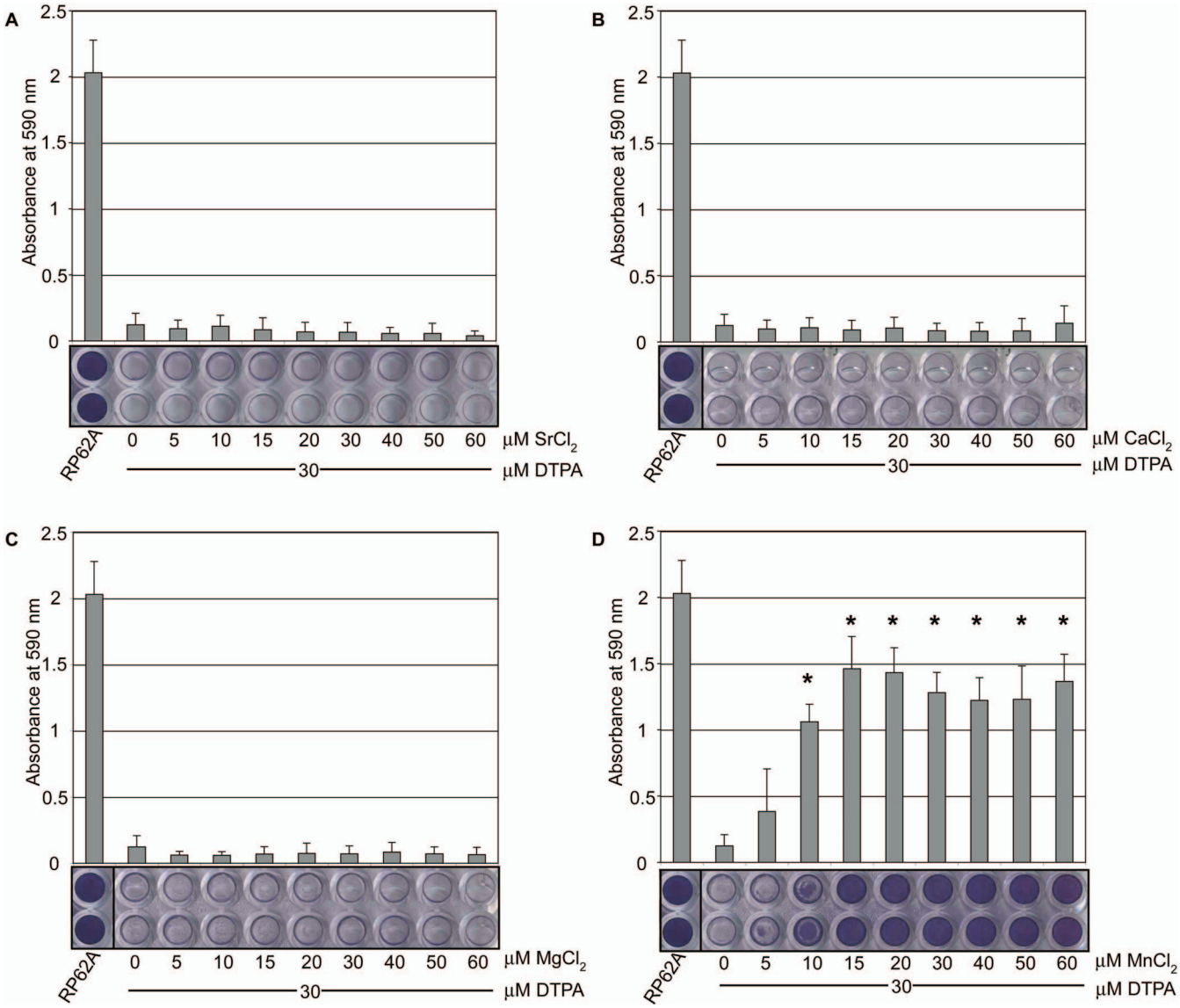

Fig. S3. Affect of Sr, Ca, Mg, and Mn on biofilm formation. (*A*) $SrCl_2$ does not reverse biofilm inhibition by 30 μM DTPA. All data at 30 μM DTPA show statistically significant decreases compared to no-treatment control (RP62A). (*B*) $CaCl_2$ does not reverse biofilm inhibition by 30 μM DTPA. All data at 30 μM DTPA show statistically significant decreases compared to no-treatment control (RP62A). (*C*) $MgCl_2$ does not reverse biofilm inhibition by 30 μM DTPA. All data at 30 μM DTPA show statistically significant decreases compared to no-treatment control (RP62A). (*D*) Addition of 10 μM or greater $MnCl_2$ effected partial rescue of biofilm formation in the presence of 30 μM DTPA. All data at 30 μM DTPA show statistically significant decreases compared to no-treatment control (RP62A). Statistically significant increases over the 0 μM $MnCl_2$/30 μM DTPA datapoint are marked with an asterisk (*, $P < 0.05$; $n = 3$). The levels of $MnCl_2$ required to rescue biofilm formation were at least 500 times higher than the concentration of Mn in serum (≈20 nM) (6), indicating that this is unlikely to be a biologically relevant phenomenon. This result may be due to competition for DTPA and release of chelated zinc. The affinity of Mn for DTPA (log $K = 15.5$) is within approximately three orders of magnitude of the Zn affinity (log $K = 18.75$), whereas the affinities of Ca, Sr, and Mg for DTPA are eight to nine orders of magnitude lower than zinc (log $K = 10.74$, 9.68, and 9.3, respectively) (7). Other divalent cations such as Fe, Co, or Ni were not tested because their affinity for DTPA equals or exceeds that of Zn. Any change in biofilm formation in the presence of these cations would be uninterpretable, as they could compete effectively with Zn for DTPA binding.

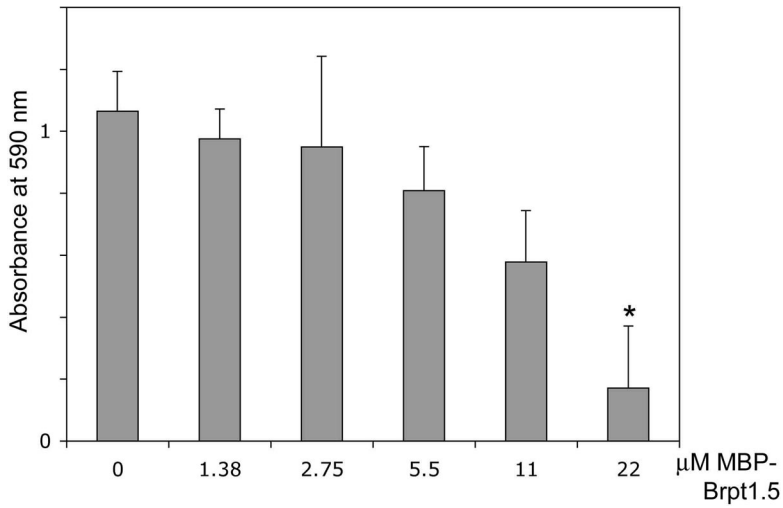

Fig. S4. Inhibition of RP62A biofilms by MBP–Brpt1.5 at 750 μM $ZnCl_2$. Dose–response of biofilm inhibition by MBP–Brpt1.5 at a fixed 750 μM $ZnCl_2$ concentration. Asterisks indicate the level of statistical significance relative to the untreated control (*, $P < 0.05$; $n = 3$).

Table S1. Circular dichroism secondary structure analyses of Brpt1.5

	% α-helix	% β-sheet	% Turn	% Coil
Brpt1.5	4	39	24	32
Brpt1.5 + 10 mM $ZnCl_2$	5	38	23	32
H75A/H85A	4	38	23	32
H75A/H85A + 10 mM $ZnCl_2$	5	40	22	32

Far-UV CD spectra were collected on samples dialyzed into 20 mM Tris, 50 mM NaF. Secondary structure content was determined using the program CDSSTR on Dichroweb. NRMSD values ranged from 0.039 to 0.043.

Table S2. Sedimentation velocity parameters for Brpt1.5

	$s^0_{20,w}$	f/f_0
Brpt1.5	1.55	2.21
Brpt1.5 + 10 mM $ZnCl_2$	2.46	1.66

Values of $s^0_{20,w}$ were determined from data at four or five concentrations. Values of the frictional ratio, f/f_0, were averaged from four or more independent experiments.

Table S3. Sedimentation equilibrium parameters for Brpt1.5 and Brpt2.5 plus $ZnCl_2$

	$M_{sequence}$		$M_{experimental}$ (95% confidence)	
	Monomer	Dimer	0 mM Zn	10 mM Zn
Brpt1.5	22,284	44,568	22,075 (19,820–24,259)	41,213 (38,823–43,536)
Brpt2.5	35,971	71,942	36,987 (34,519–39,380)	78,541 (76,220–80,863)

K_d for monomer–dimer association

	2 mM Zn	5 mM Zn	10 mM Zn
Brpt1.5	113 μM (62.8–200 μM)	5.06 μM (3.59–7.08 μM)	0.353 μM (0.196–0.647 μM)
Brpt2.5	25.5 μM (17.8–36.8 μM)	0.072 μM (0.165–0.0322 μM)	ND*

Confidence intervals (95%) were calculated by WinNONLIN. $M_{sequence}$ is the molecular weight determined by ProtParam from the amino acid sequence. $M_{experimental}$ is determined from global analysis of sedimentation equilibrium curves.
*Not determined; no detectable monomer was observable under this condition, precluding the determination of an equilibrium constant.